

TABLE S1: Characteristics of non-diabetic and STZ-induced diabetic C3H and Hcb-19 mice

Characteristics	C3H wildtype(WT)		Hcb-19 (TxNIP mutant)		p-value
	Non-diabetic	Diabetic	Non-diabetic	Diabetic	
Glycemia (mmol/L)	8.3±0.7	33.3±0***	5.4±1.1***	33.1±0.5###	***p<0.0001 vs WT non Diabetic, ###p<0.0001 vs Hcb19 non-diabetic
Body weight (g)	21±1.5	20±0.7	32±1.5***	21±2.1###	***p<0.0001 vs WT non Diabetic, ###p<0.0001 vs Hcb19 non-diabetic
Left kidney weight (mg)	191±28.3	234±23.4	303±20.6***	256±35.1##	***p<0.0001 vs WT non Diabetic, ##p<0.001 vs Hcb19 non-diabetic
Left kidney weight/body weight	9.4±0.7	12.5±1.8*	9.4±0.2	13.3±0.9###	*p<0.01 vs WT non Diabetic, ###p<0.0001 vs Hcb19 non-diabetic
Albumin/ Creatinine ratio (µg/mg)	28.4±16.8	384.8±184.4***	212.9±83.4***	217.5±84.9***	***p<0.0001 vs WT non Diabetic

Results are expressed as mean±SD

FIGURE S1. Renal parameters of STZ-diabetic and non-diabetic TxNIP^{+/+} (WT), TxNIP^{-/-} (KO) and TxNIP^{+/-} (HET). Assays were performed as described in Methods after 24 weeks of diabetes. (A) 24h urine albumin excretion (μg), (B) urine albumin/creatinine ratio ($\mu\text{g}/\text{mg}$), (C) 24h proteinuria (μg) and (D) Serum Cystatin C (pg/mL). Results are expressed as mean \pm SE (n= 6-7 mice/condition). * $p<0.05$ diabetic WT vs non-diabetic WT, diabetic KO and diabetic HET, ** $p<0.01$ diabetic WT vs non-diabetic WT and diabetic KO, and *** $p<0.001$ diabetic WT vs non-diabetic WT.

FIGURE S2. TxNIP mRNA content of renal cortex. TxNIP^{+/+} (WT), TxNIP^{-/-} (KO), and TxNIP^{+/-} (HET) mice were rendered diabetic or not with STZ as in Methods. Renal cortex TxNIP mRNA was determined by real time RT-PCR and corrected for *actb* and normalized to nondiabetic WT. Results are mean \pm SE from 3-5 mice/condition. ** $p<0.01$ diabetic HET vs non-diabetic WT and diabetic KO, *** $p<0.001$ diabetic WT vs non-diabetic WT and diabetic KO, ## $p<0.01$ diabetic HET vs non-diabetic HET.

FIGURE S3. Mesangial matrix expansion, glomerular fibrosis, Nox4 expression and Electron Micrographs from nondiabetic and STZ-induced diabetic C3H and Hcb-19 mice. (A) Representative images of Periodic Acid Schiff (PAS) stained glomeruli. (B) Quantitation of mesangial matrix expansion from PAS stained sections as described in Methods. (C) Collagen IV IHC. (D) Quantitation of collagen IV as percentage of glomerular area. (E) TGF β 1 staining. (F) Quantitation of TGF β 1. (G) Nox4 IHC in glomeruli. (H) Quantitation of Nox4. Results are expressed as mean \pm SD, n=4-5mice/condition. * $p<0.05$ diabetic C3H vs nondiabetic C3H and nondiabetic Hcb19 vs nondiabetic C3H. # $p<0.01$ diabetic C3H vs diabetic Hcb-19. (I) Representative electron micrographs (magnification x 15,000) of glomeruli from non-diabetic and diabetic C3H and Hcb-19 mice where arrows= slit diaphragm, *FP= foot process and GBM=glomerular basement membrane.

FIGURE S4. Histopathological markers of renal fibrosis in STZ-diabetic and non-diabetic TxNIP^{+/+} (WT), TxNIP^{-/-} (KO) and TxNIP^{+/-} (HET) mice. Representative images of markers of fibrosis in non-diabetic and STZ-diabetic HET mice assessed by collagen IV (A, B), TGF β (C, D), and renal interstitial fibrosis (Masson's Trichrome staining) (E,F). Staining of mesangial matrix was assessed with PAS (G, H). Quantitation of the staining is shown in the graphs in the bottom panels (I-L). HET (n=3 mice/condition), WT and KO (n=5 mice/condition). Results are means \pm SE; * $p<0.05$ diabetic WT vs non-diabetic WT and diabetic KO, ** $p<0.01$ diabetic WT vs non-diabetic WT and diabetic HET, and *** $p<0.001$ diabetic WT vs non-diabetic WT, diabetic KO and diabetic HET.

FIGURE S5. Expression of nephrin in glomeruli. (A) Representative images of nephrin staining (IHC) in glomeruli from nondiabetic and diabetic WT and TxNIP KO mice. Quantitation is shown in the graphs in the bottom panel (n=4 mice/condition). Results are means \pm SE relative to WT designated as 1.0; * $p<0.05$ diabetic WT vs diabetic KO and *** $p<0.001$ diabetic WT vs non-diabetic WT.

FIGURE S6. Morphological EM changes in glomerular basement membrane and podocyte foot process. (A) Representative electron micrographs (magnification approx. x15,000) of non-diabetic and diabetic TxNIP^{+/-} (HET) mice where arrows= slit diaphragm, *FP= foot process and GBM=glomerular basement membrane. (B) Quantification of GBM thickness, and (C) podocyte foot process effacement

quantified as in Methods from 9 different fields from each of 3 mice/condition. Results are expressed as means \pm SE. * p <0.01 diabetic WT vs non-diabetic WT and diabetic KO, *** p <0.001 diabetic WT vs non-diabetic WT, diabetic KO and diabetic HET.

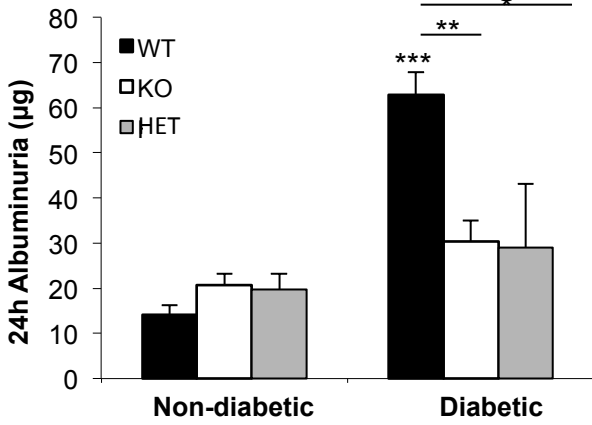
FIGURE S7. Markers of oxidative and nitrosative stress and Nox4 expression. Representative images of glomerular nitrosative stress in non-diabetic and diabetic TxNIP^{+/-} HET mice, as indicated by glomerular nitrotyrosine staining (A,B), and its quantification (E) (n=3-5 mice/ condition). Representative images of glomerular Nox4 expression in HET mice (C,D) and its quantification (F) (n=3-5 mice/condition). Results are means \pm SE. ** p <0.001 diabetic WT vs non-diabetic WT and diabetic KO, and *** p <0.001 diabetic WT vs non-diabetic WT and diabetic KO, # p <0.01 diabetic HET vs non-diabetic HET, and ^{ss} p <0.001 diabetic HET vs diabetic KO. (G) ROS detected as 24h urinary 8-hydroxy-2-deoxy-guanosine levels (pg) from 3-7 mice/condition. (H) Expression of *Nox4* mRNA, corrected for the housekeeping gene, *actb*, and normalized to non-diabetic WT in renal cortex. Results are means \pm SE (n=3-5 mice/condition). * p <0.05 diabetic WT vs non-diabetic WT and diabetic KO, ** p <0.01 diabetic KO vs non-diabetic KO and diabetic WT, *** p <0.001 diabetic WT vs non-diabetic WT and diabetic HET, and # p <0.01 diabetic HET vs non-diabetic HET.

FIGURE S8. Oxidative and nitrosative stress in tubular cells. (A) Representative images of tubular Nox4 and RNS as indicated by nitrotyrosine staining (n=3 mice/ condition). Quantitation of tubular (B) Nox4 and (C) Nitrotyrosine . Results are mean \pm SE. * p <0.05 diabetic WT vs non-diabetic WT and diabetic TxNIP KO.

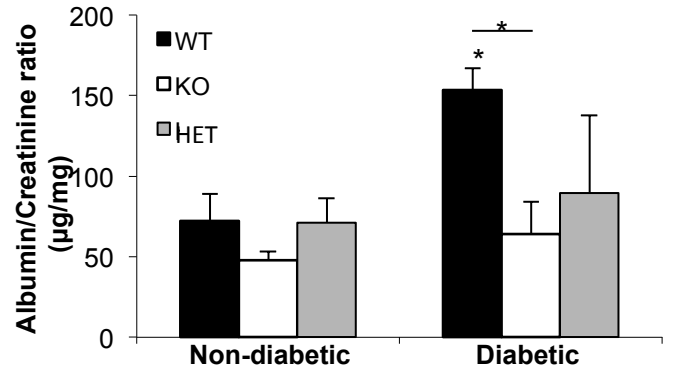
FIGURE S9. Markers of glomerular inflammation. (A) Representative images of glomerular inflammation indicated by F4/80 staining in glomeruli from non-diabetic and diabetic TxNIP^{+/-} (HET) mice. Quantification of staining intensity is shown in the right panel. Expression of (B) *IL1 β* and (C) *TNF α* mRNA corrected for the housekeeping gene *actb*, and normalized to non-diabetic WT in renal cortex. Results are mean \pm SE (n= 3-5 mice/ condition) * p <0.05 diabetic WT vs non-diabetic WT, diabetic KO and diabetic HET, ** p <0.001 diabetic WT vs non-diabetic WT and diabetic KO, and ^s p <0.05 diabetic HET vs non-diabetic HET.

Figure S1

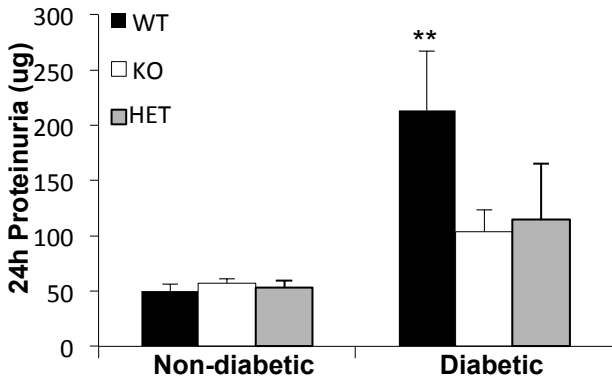
A



B



C



D

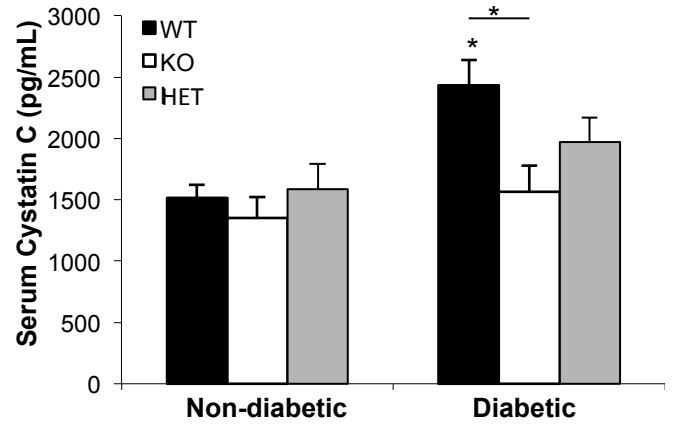


Figure S2

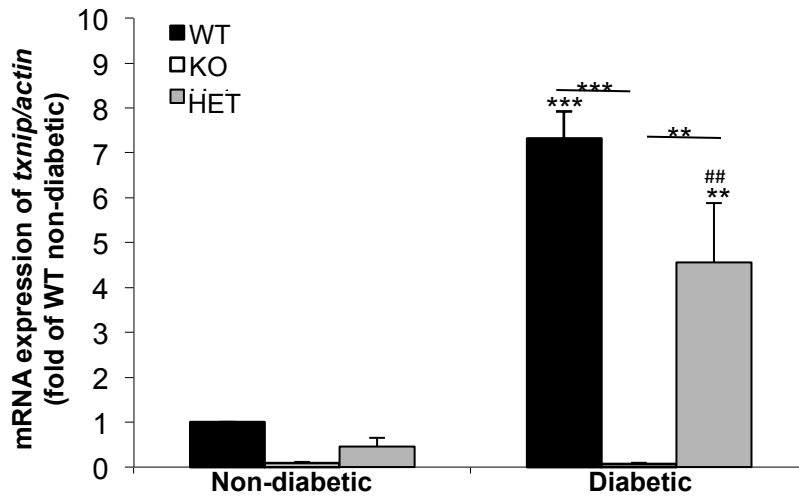


Figure S3

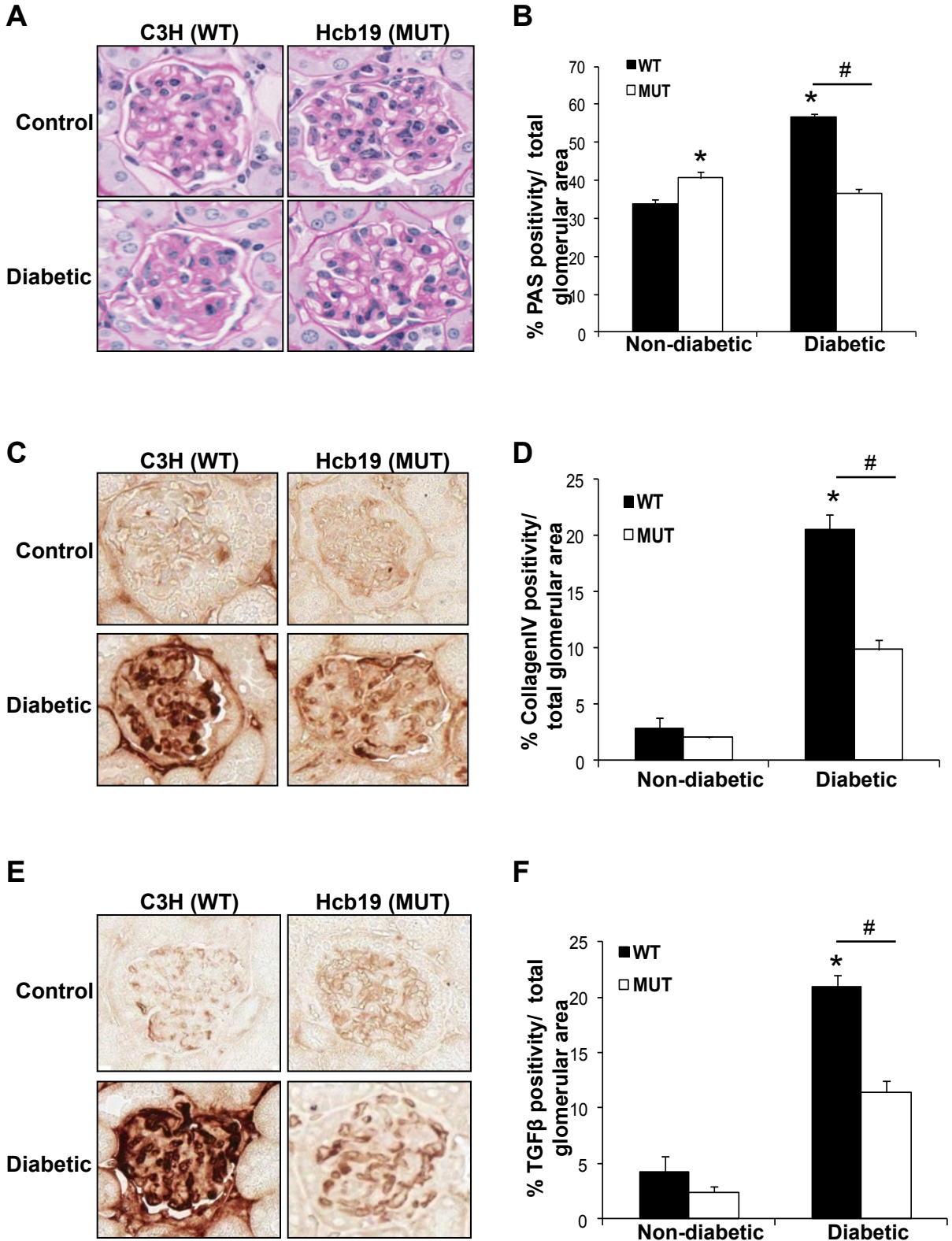


Figure S3

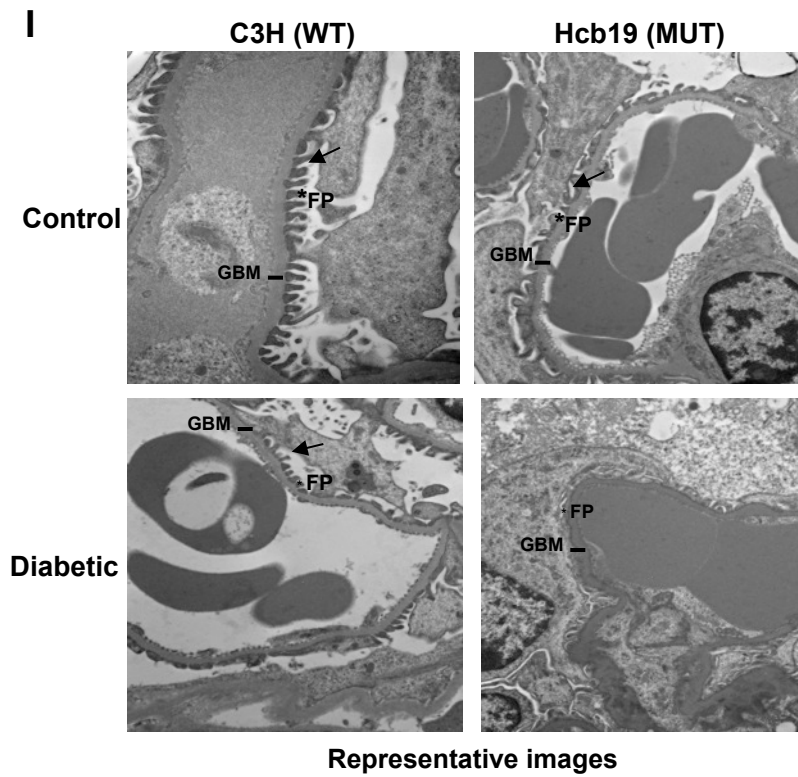
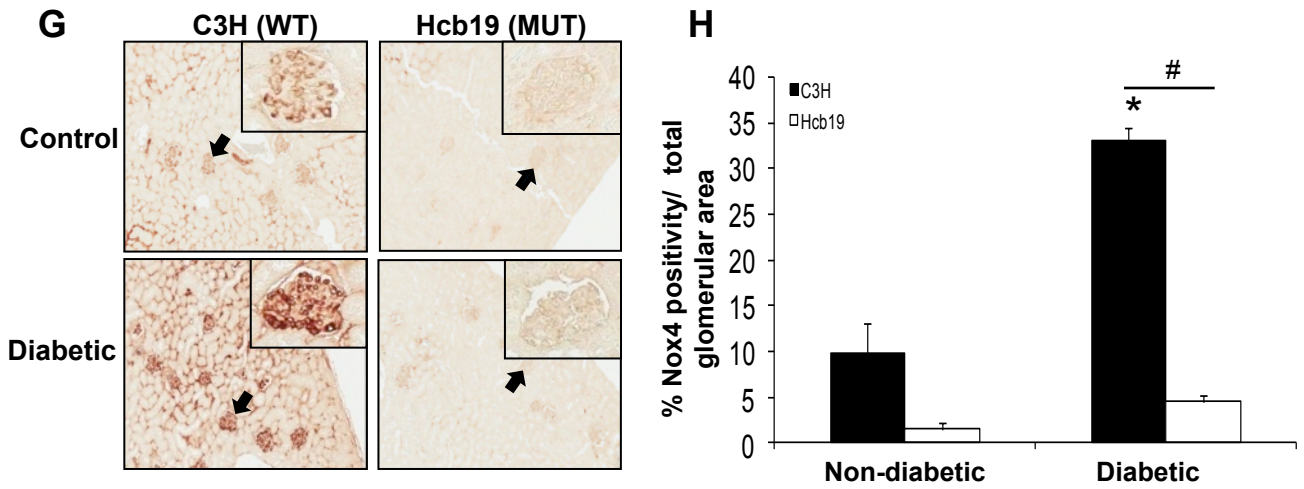


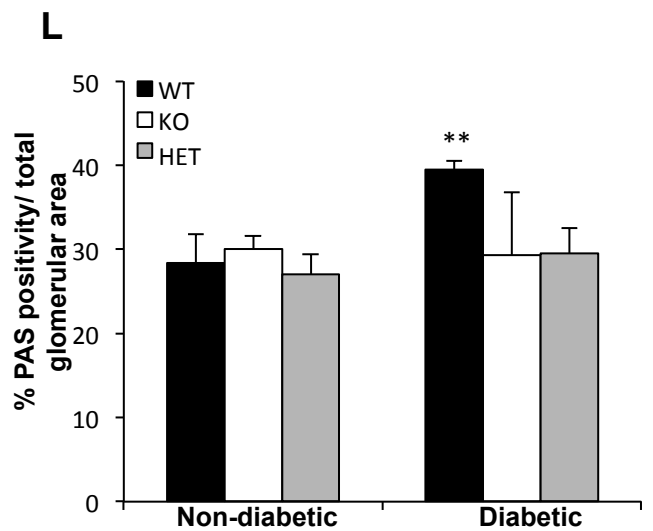
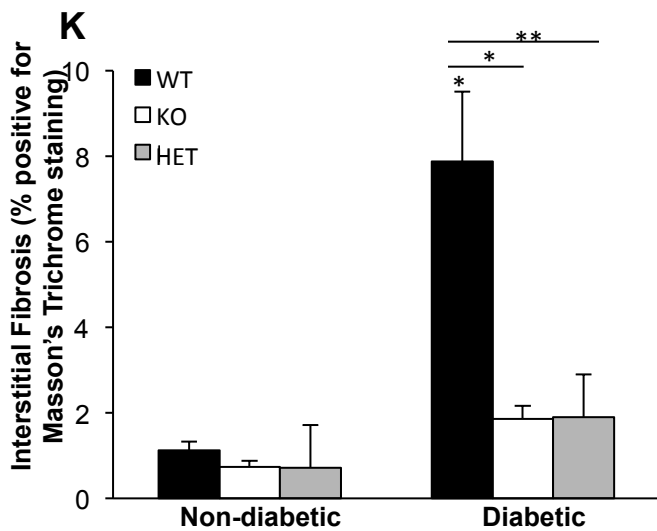
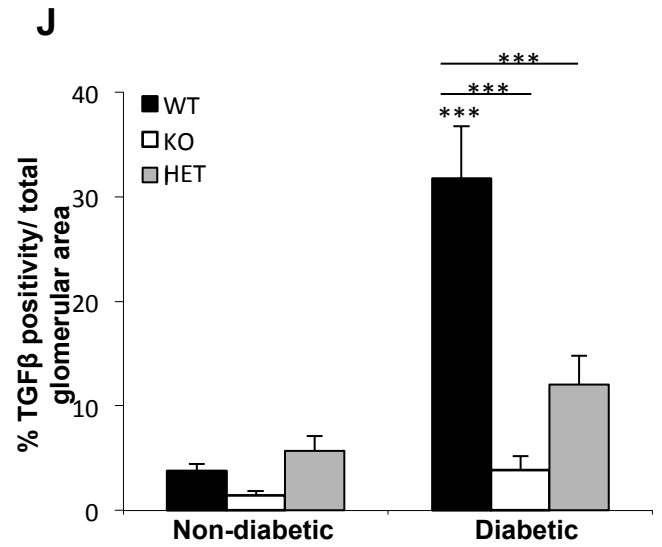
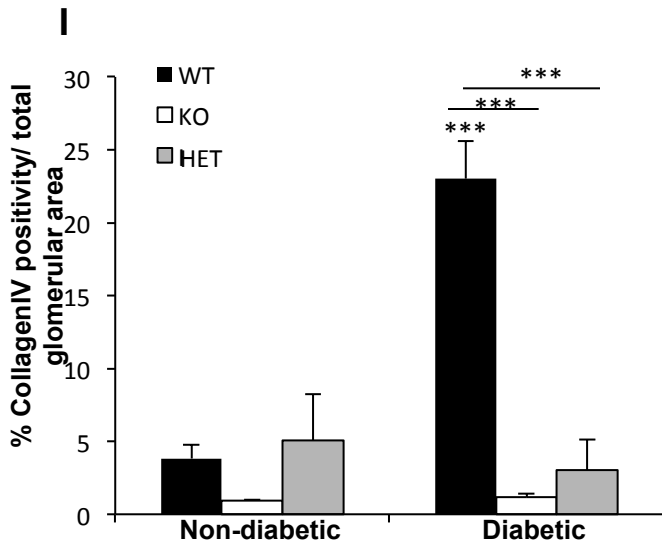
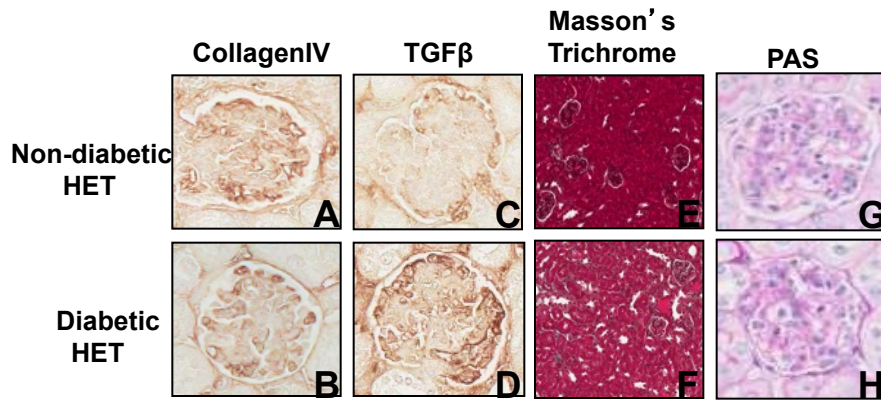
Figure S4

Figure S5

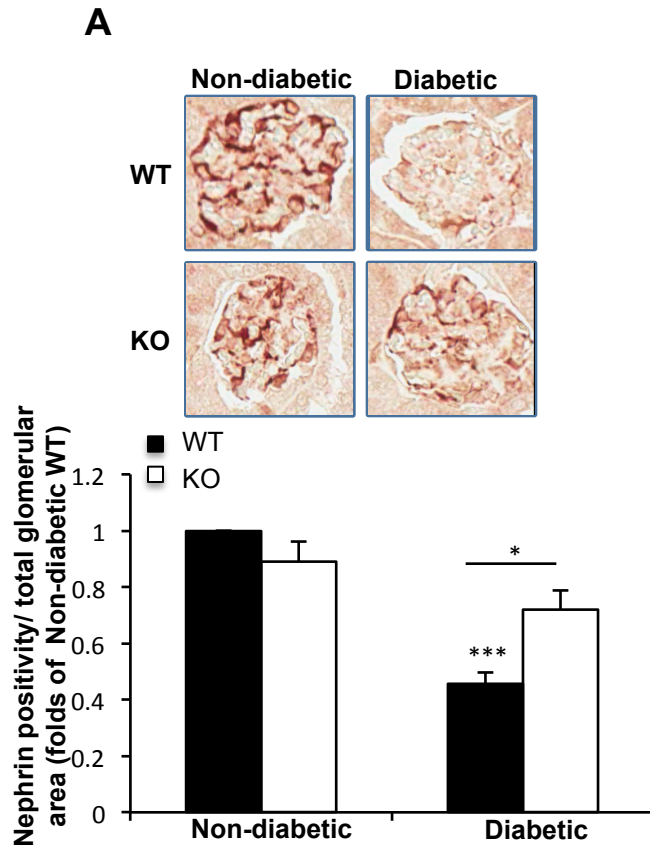
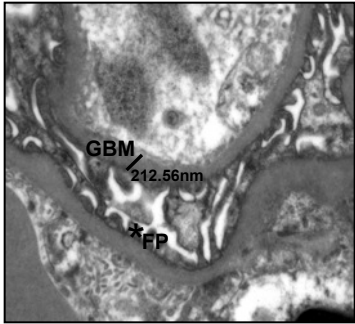


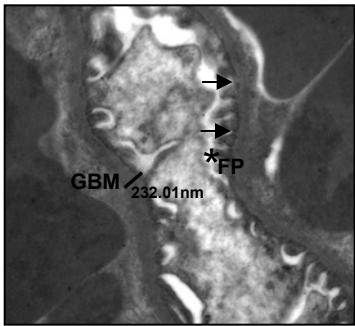
Figure S6

A

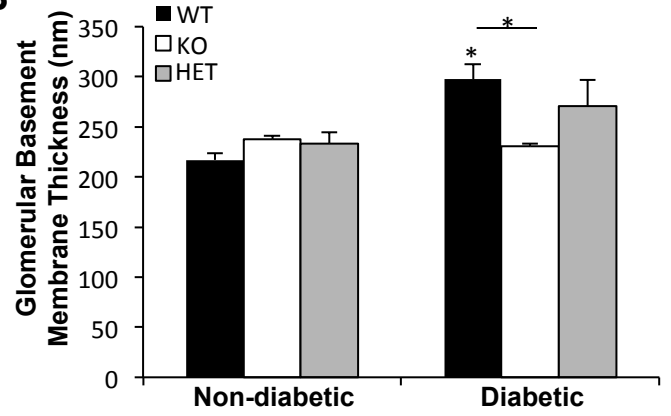
Non-diabetic
HET



Diabetic
HET



B



C

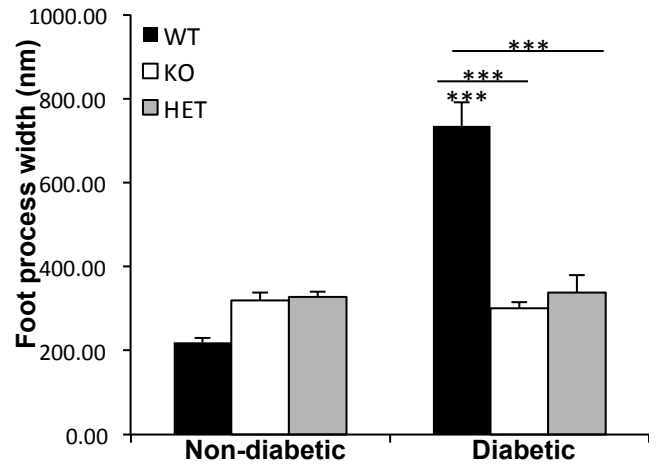


Figure S7

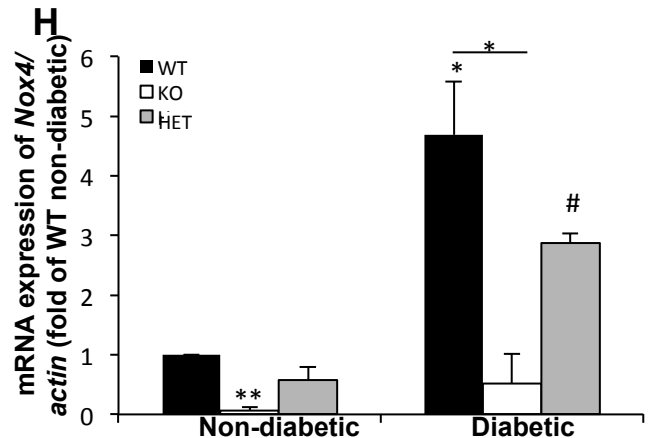
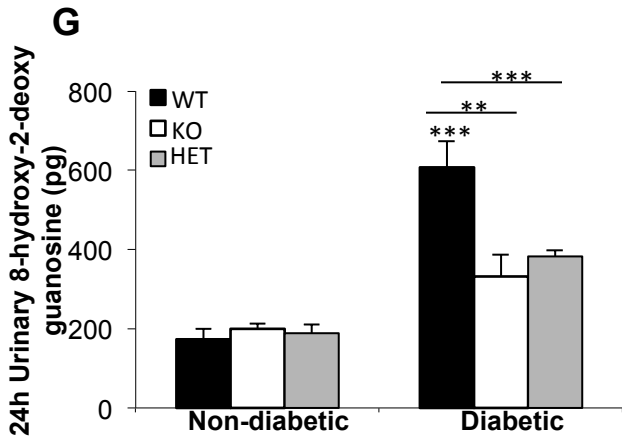
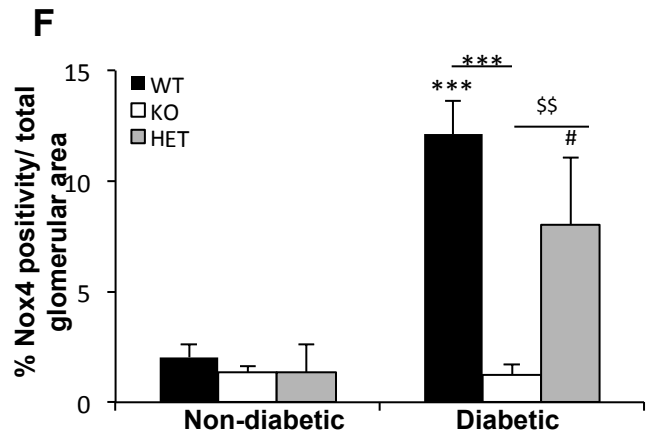
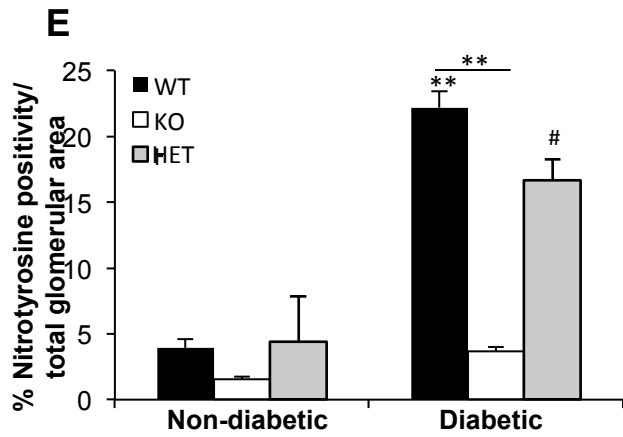
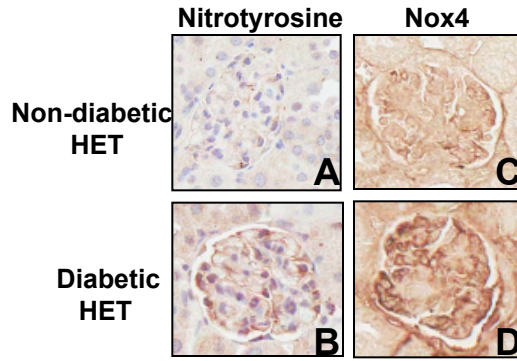
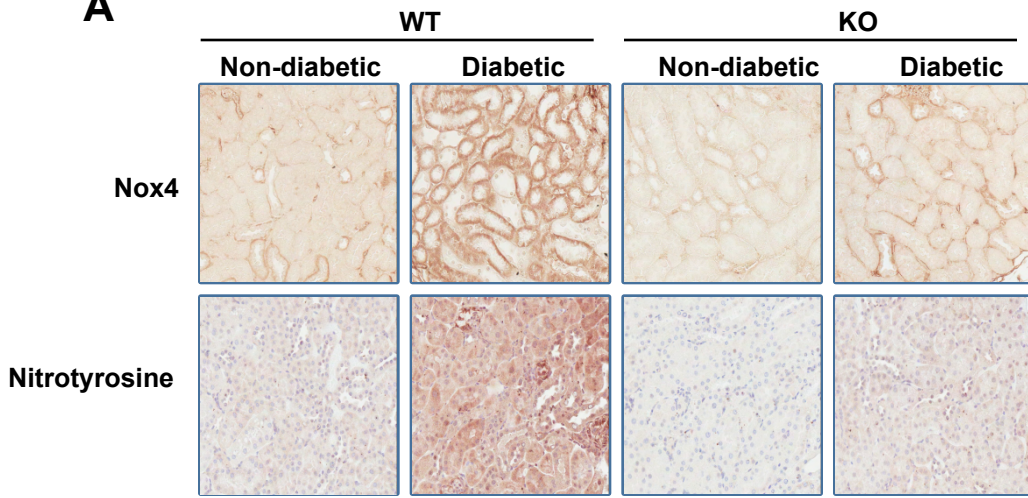
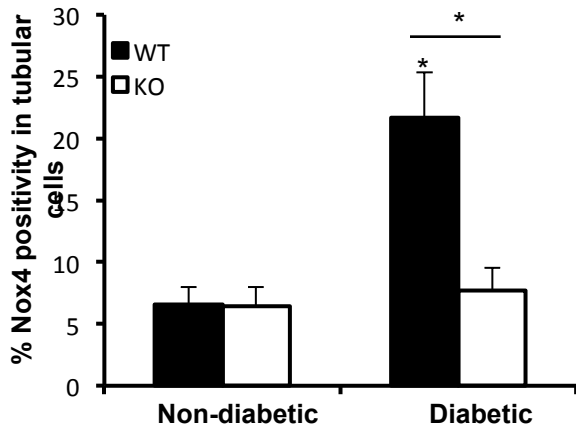


Figure S8

A



B



C

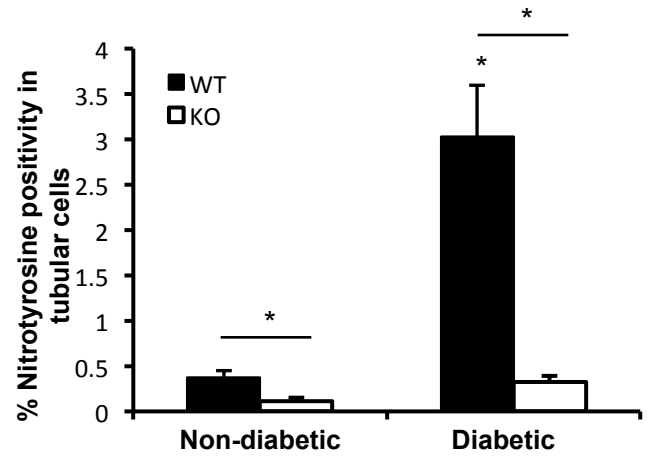
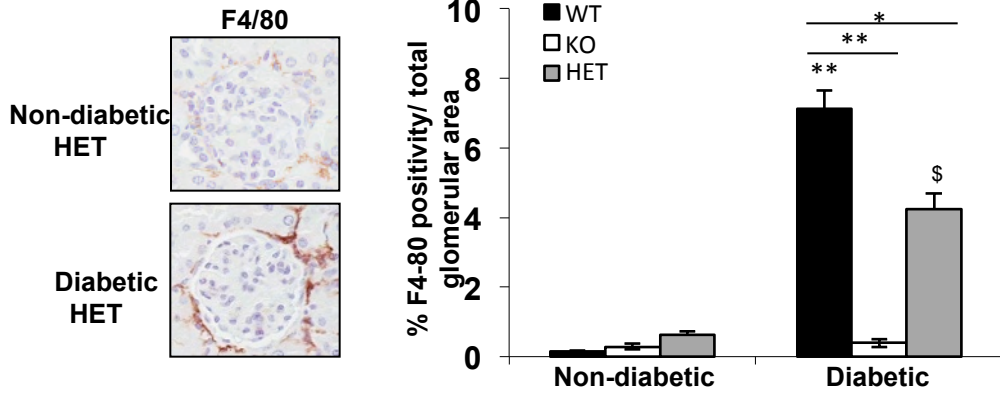
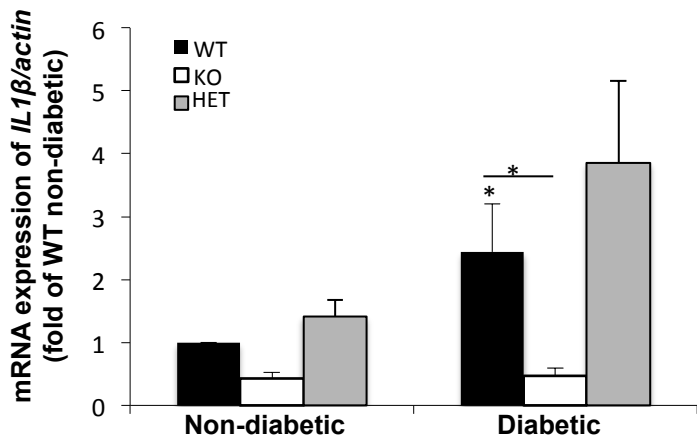


Figure S9

A



B



C

